J Fluoresc (2012) 22:849–855
DOI 10.1007/s10895-011-1019-8

ORIGINAL PAPER

The pH Dependence of the Total Fluorescence of Graphite Oxide

Sven Kochmann · Thomas Hirsch · Otto S. Wolfbeis

Received: 19 August 2011 / Accepted: 21 November 2011 / Published online: 6 December 2011

Abstract Graphite oxide was characterized by pH dependent excitation-emission matrices from 300 to 500 nm in excitation and from 320 to 600 nm in emission which reveal the presence of two pH steps. These are assigned to the presence of carboxy groups and phenolic hydroxy groups, respectively. Fluorescence is strongest at 470 nm excitation and 555 nm emission. The fluorescence intensity is a function of pH but not of temperature, and is not quenched by oxygen.

Keywords Graphite oxide · pH-dependence · Fluorescence · Excitation-emission matrix · Nano materials

Introduction

Graphene consists of a single sheet of sp^2-hydridized carbon atoms and therefore provides the highest possible surface to volume ratio [1]. It is most suitable for electronical sensing due to its high conductivity [2] and quantum Hall effect at room temperature [3] which provide the possibility of highly sensitive detection of gases [4, 5].

Graphite oxide (GO), a product of the oxidation of graphene, is characterized by a disturbed sp^2-system due to the presence of various oxygen functional groups [1]. However, GO is not a well defined nor consistent material. This is mainly due to the use of different methods of preparation which employ various types and quantities of oxidation agents [6]. In fact, the term "graphite oxide" refers to a whole set of materials that can be distinguished with respect to flake size, oxidation level, and number of layers. These parameters primarily control the number of functional oxide groups on the surface and the edge, but also allow GO to interact with many types of other materials, e.g. DNA [7] and amines [8]. The hydrophilic character of these groups allows the preparation of stable aqueous solutions of GO. This makes the material compatible with spin-on or dropcast techniques to deploy thin films.

The oxidation level of GO introduces a band gap which enables photoluminescence to occur [9, 10]. By tuning size, oxidation level and number of layers it is possible to create materials with specific optical, electrical and mechanical properties [11, 12]. The photoluminescence of GO has only sparsely been examined [9, 10, 13]. Eda et al. have photoexcited GO at 325 nm and observed a blue luminescence [14]. Chen et al. examined the pH-dependence of the fluorescence and the effect of the ionic strength in the visible and near-infrared spectrum [15]. We are presenting here a systematic study on the multiple fluorescence of GO and its dependence on excitation wavelength, emission wavelength and pH value in the near-UV and visible part.

Materials and Methods

All chemicals except graphite were purchased from Merck (Darmstadt; www.merck.de). They were of analytical grade and used without further purification.

S. Kochmann · T. Hirsch (✉) · O. S. Wolfbeis
Institute of Analytical Chemistry, Chemo- and Biosensors, University of Regensburg, 93053 Regensburg, Germany
e-mail: thomas.hirsch@chemie.uni-regensburg.de

Graphite (99%) was from Thielmann Graphite GmbH (Grolsheim; www.kwthielmann.de). In the following procedure high concentrated acids (corrosive) and oxidation agents are used which require careful handling and appropriate protective equipment (goggles, coat, gloves).

Graphite was oxidized by a modified Hummers method to obtain water-soluble graphite oxide (GO) [16]. Briefly, graphite (100 mg) and sodium nitrate (100 mg) were added into 5 mL of fuming sulfuric acid (97%). Then, solid potassium permanganate (1 g) was slowly added to form the green manganate dimer (Mn_2O_7). The mixture was stirred for 3 days, slowly diluted with sulfuric acid (5%; this has to be done with extreme caution; the process is highly exothermic) and heated for 3 h to about 100 °C. (Safety note: The previous steps have to be performed with extreme caution and under a hood. The use of safety goggles and gloves is mandatory.) After slow addition of 1 mL of hydrogen peroxide (30%), the resulting solid was collected by centrifugation and washed five times with sulfuric acid (3%) and hydrogen peroxide (3%), two times with hydrochloric acid (3.7%) and two times with water. Ions remaining in the solution were removed by dialysis against ultrapure water (3 days; water was changed every day). The water was removed by lyophilization to yield ~50 mg of water-soluble GO in the form of a light brown powder which was used without any further purification.

GO ethyl ester (GOEE) was prepared by adding 1-Ethyl-3-(3-dimethylaminopropyl)carbodiimide (5.0 mg), N-Hydroxysuccinimide (2.8 mg) and ethanol (1 mL) to a solution of GO (5 mL; 0.5 mg mL^{-1}) [17]. The solution was stirred at room temperature for 12 h. Remaining ions and agents were removed by dialysis against ultrapure water (3 days; water was changed every day). This solution was diluted (1:40) with the corresponding buffer solutions.

Britton-Robinson buffers (10 mmol L^{-1}) of varying pH values were used in all measurements. The pH values were adjusted by adding NaOH (1 M) and HCl (1 M), respectively. GO was dissolved in the corresponding buffer solutions to get a final concentration of GO in all solutions of 0.1 mg mL^{-1}. The pH values of solutions were checked with a digital pH meter type *CG 842* (SI Analytics GmbH, www.si-analytics.com) calibrated with standard buffers of pH 4.00 and pH 7.00 (Carl Roth, Karlsruhe, www.carlroth.com) at 21 °C, 37 °C and 60 °C. Luminescence spectra were acquired on a *Aminco Bowman Series 2* (Thermo Spectronic; www.thermo.com) luminescence spectrometer with *AB2 Luminescence Spectrometer V 5.30* software. UV/Vis spectra were acquired on a *Varian Cary 50 Bio* (Agilent Technologies; www.varianinc.com),

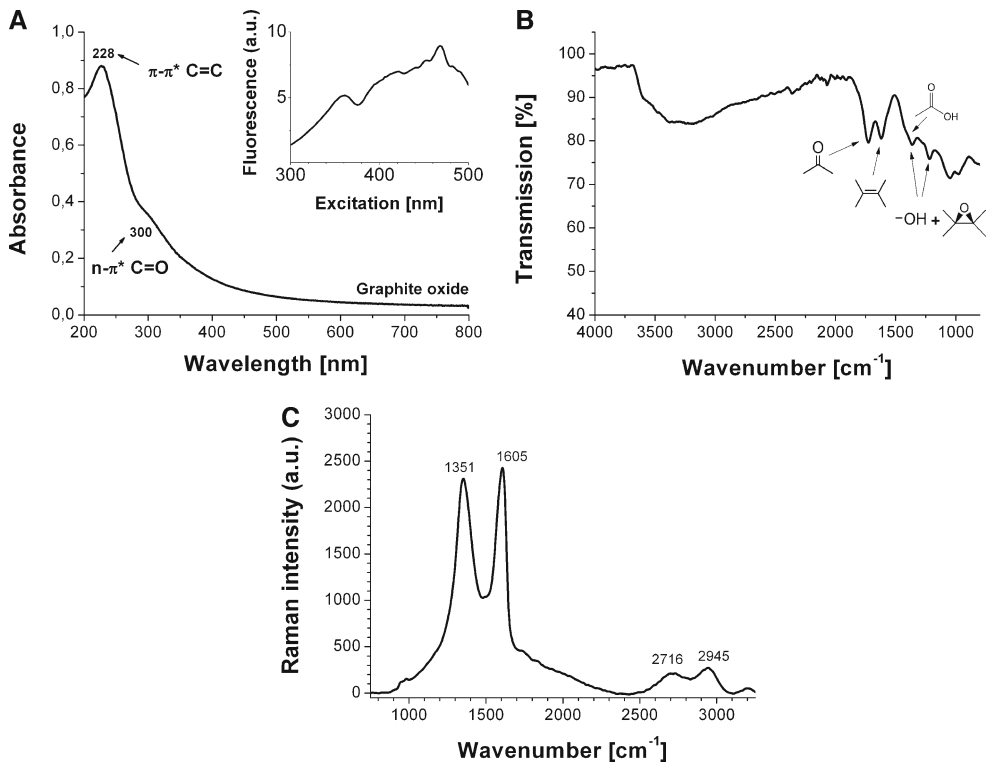

Fig. 1 UV/Vis (**A**) and infrared spectrum (**B**) of graphite oxide revealing the presence of various oxygen functions. The inset shows the excitation spectrum at 555 nm emission. Raman spectrum (**C**) of GO showing the G (1605 cm^{-1}), D (1351 cm^{-1}) and 2D (2700–2950 cm^{-1}) peak (see text)

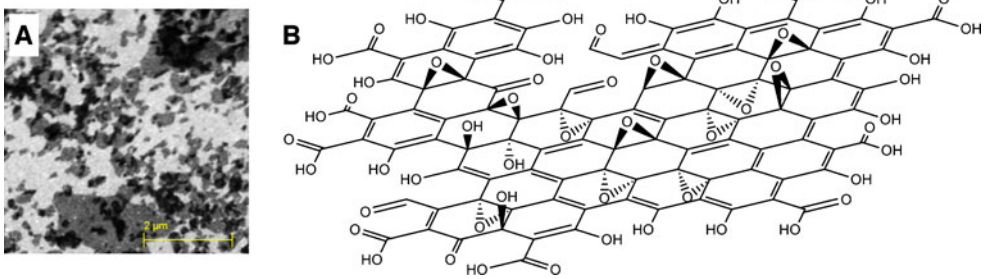

Fig. 2 (**A**) SEM picture of GO revealing the size and shape distribution. (**B**) Suggested structure model of GO showing its functional oxygen groups. The model shows the actual C:O ratio but it does not represent a whole flake

FT-IR spectra on an *Excalibur FTS 3000 Mx* (Bio-Rad Laboratories; www.bio-rad.com) and Raman spectra on a *DXR Raman-Microscope* (532 nm, 8 mW CW, Thermo Fisher Scientific; www.thermofisher.com).

Each excitation/emission matrix EEM was obtained by incrementing the excitation wavelength from 300 to 500 nm in 2-nm-steps. The respective emission spectra were scanned at an offset of 20 nm from the excitation wavelength up to 600 nm in 1-nm-steps. The fluorescence intensities at various pH values strongly differ, so that the sensitivity of the detector for each pH had to be adjusted. Except for pH 10.1, the sensitivity was set in such a way that the intensity at 470/550 nm was about 85% of the maximum signal of the detector. The maximum sensitivity of the detector has been used at pH 10.1.

Characterization of the Graphite Oxides Studied

It is known that graphite oxide (GO), even if prepared under virtually identical conditions, can strongly vary in terms of functional groups and its elementary composition, in particular with respect to carbon and oxygen. Elementary analysis of GO prepared by the Hummers method reveals a C:O ratio of 100:56. This implies that about every second carbon atom is linked to an oxygen atom! The UV absorption spectrum of GO exhibits one broad band with a maximum at 228 nm and a shoulder at 300 nm which can be assigned to the π-π^* transition of C=C and the n-π^* transition of carbonyl groups, respectively (Fig. 1A). The absorption then slowly decays but extends towards into the visible. This is causing the brown color. The FT-IR spectrum (Fig. 1B) indicates the presence of aldehydes and/or ketones (at 1728 cm^{-1}) and of aromatic C=C double bonds (at 1618 cm^{-1}). Weaker bands can be found that are assigned to hydroxy (1364 cm^{-1}) and epoxy (1225 cm^{-1}) groups. The broad band between 2866 cm^{-1} and 3607 cm^{-1} indicates the presence of aliphatic and aromatic C-H and O-H stretch vibrations [18]. The graphene-like "honeycomb" structure is confirmed by Raman data (Fig. 1C), the vibrations of the hexagonal lattice of GO giving a band at 1605 cm^{-1} (G band) along with two disordered bands at 1351 cm^{-1} (D band) and 2700 – 2950 cm^{-1} (2D band; overtone of D) [19]. The SEM image of the material (Fig. 2A) reveals the inhomogeneous size of the individual flakes with diameters from 100 nm up to 2 µm. These results lead to the structure model given in Fig. 2B showing

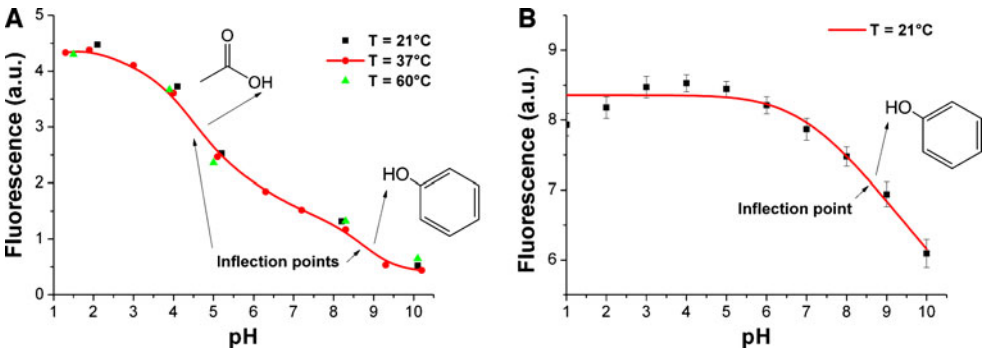

Fig. 3 (**A**) Fluorescence intensity (exc/em 470/555 nm) of GO (0.1 mg mL^{-1}) plotted as function of the pH value of the solution at various temperatures. The two inflection points are assigned to the dissociation of the carboxy groups (at 4.5) and the phenolic hydroxy groups (at 8.8), respectively. (**B**) If GO is converted into its ethyl ester, the first inflection point disappears. The GO ethyl ester also is less soluble in water at lower pH values which results in lower total fluorescence intensity (pH 1 and 2)

its functional oxygen groups: ketones, aldehydes, epoxides, hydroxy groups and carboxylic acids.

Fluorescence of GO

The pH dependence of the fluorescence of GO in water solution at fixed excitation/emission wavelengths of 470/555 nm was studied first. Figure 3A shows that pH exerts a large effect. At pH 1.5, the intensity is about 10 times higher than that at pH 10.1. Inflection points can be identified in the titration plots at pH 4.5 and 8.8. The first one can be assigned to the dissociation of carboxy groups, and the second one to the dissociation of aromatic hydroxy groups, respectively. This is in agreement with the model of GO shown in Fig. 2B, and with related models [20]. In order to prove that the carboxy group is responsible for the transition at around pH 4.5 (the typical pK_a value of aromatic carboxy acids), we have converted GO into its ethyl ester (GOEE) as described in the experimental part. Indeed, the plot for GOEE has only one inflection point at pH

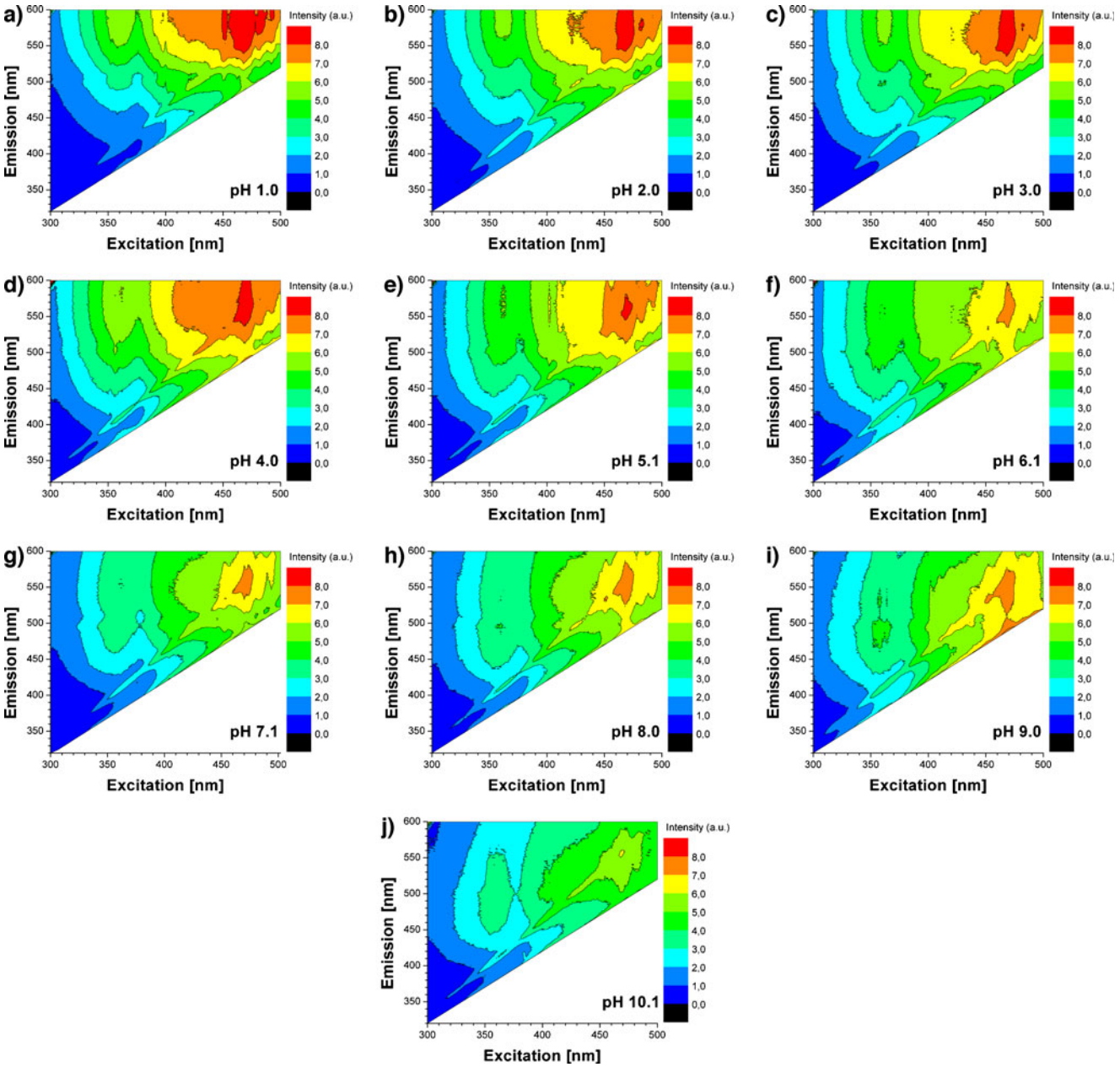

Fig. 4 Excitation-emission matrices of graphite oxide at pH values from 1.0 to 10.1

8.8 (see Fig. 3B) that can be assigned to the phenolic hydroxy groups of GO.

Temperature exerts a minimal effect (only about 2%) on fluorescence intensity between 20 and 60 °C. Oxygen does not act as a quencher.

The absorption spectrum of graphite oxide (see Fig. 1A) is typical for species where numerous transitions occur in parallel. The shoulder at around 300 nm is typical for the n-π^* transitions which invariably occur at about this wavelength, are rather weak in intensity, and result from the various kinds of carbonyl groups present in GO. They easily undergo intersystem crossing to a triplet state and do not cause strong fluorescence in general. Transitions of the π-π^*-type, in contrast, are highly variable in terms of wavelength and intensities. They can occur anywhere between 220 and 600 nm and lead to S_1 states that can undergo various kind of deactivation. Aside from vibrational deactivations, these include intersystem crossing, hydrogen bond deactivation (such as diabatic photodissociation of hydroxy groups), intra- and intermolecular energy transfer, and/or quenching. We also assume that flakes of GO (or sections thereof) can quench (sections of) other flakes. It is virtually impossible to identify the π-electron system that is causing the fluorescence peaks observed, in particular the strong ones located at excitation/emission wavelengths of 360/580 nm and 470/560 nm [21, 22].

In order to obtain a complete picture of the complex luminescence of GO, the excitation-emission matrices (EEM) of GO were acquired at pH values between 1.0 and 10.1 and are shown in Fig. 4. EEMs are a valueable tool to characterize materials with complex intrinsic fluorescence. These have been used before to characterize materials like human tissue [23], serum [24], diesel fuel [25], crude oil [26] and water samples [27, 28]. The EEMs of GO display a broad maximum at 470 nm excitation and 560 nm emission at any pH value. A small peak can be observed at 360 nm excitation and 580 nm emission if the pH is lower than 4. The peak disappears at pH values above 4, and another one arises at 360 nm excitation and 500 nm emission. The EEMs also contain Raman bands shifted from the excitation wavelength by 3328 cm^{-1} and caused by water.

Discussion

It is interesting to compare the fluorescence of GO with that of other carbon nanomaterials. C_{70} fullerene displays a red emission when excited with blue light (470 nm) [29]. Its fluorescence is extremely efficiently quenched by oxygen, thus enabling oxygen imaging on the ppb level [30]. Carbon nanotubes excited with red light (785 nm) emit in the near infrared area [31] which was shown to enable glucose sensing [32]. Carbon nanoparticles also display strong fluorescence [13, 33, 34] and this may be used for purposes of bioimaging [35, 36].

GO is a comparatively inhomogeneous material. A comparison of absorbance and excitation spectra (see Fig. 1A) reveals that only a small fraction exhibits luminescence while the major fraction does not. It is manifest to assume that the bulk material actually suppresses this luminescence as quantum yields are quite low. Therefore, GO is rather used in quenching applications [7, 37].

Figure 3 reveals that the pH dependent fluorescence of GO has two inflection points which are assigned to the carboxy acid and the aromatic hydroxy groups.

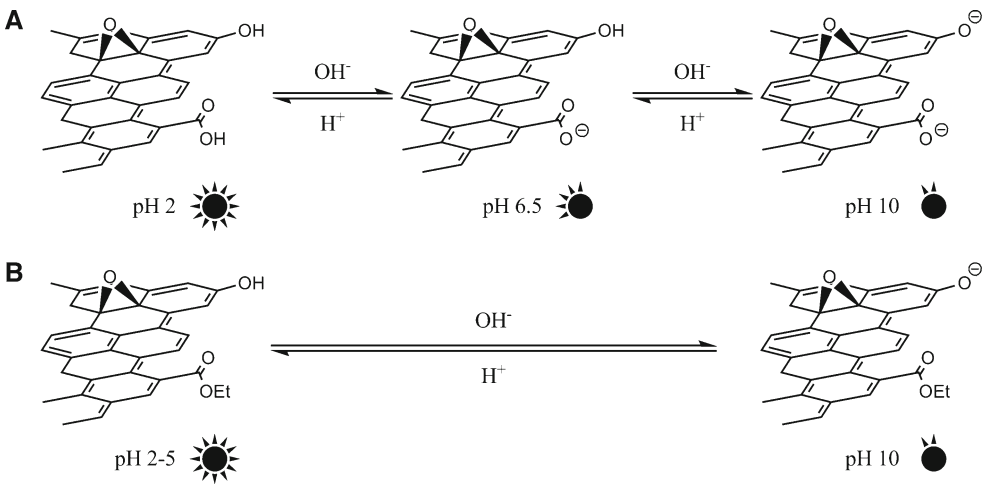

Fig. 5 (**A**) Model showing the effect of the pH on the acid-base equilibria of GO. The symbols indicate the relative fluorescence intensity of the corresponding species. (**B**) Equilibrium after conversion of the carboxy groups into their ethyl esters

The monoprotic equilibrium of GO suggested by Chen et al. [15] therefore has to be extended as there are three rather than two main forms of GO at different pH values (see Fig. 5A). GO is completely protonated at pH values < 3, and displays maximal fluorescence. From pH 3 to 6 the carboxy acid group becomes deprotonated. The fluorescence intensity decreases to 40% (at pH 6–7). At pH values > 7, the aromatic hydroxy group becomes deprotonated which results in a drop of fluorescence intensity to 15%. One conclusion of this observation is that GO is negatively charged at pH values of greater than 4. This is supported by the fact that esterification of the carboxy acid groups leads to only one inflection point (Fig. 3B) and therefore to a monoprotic equilibrium (Fig. 5B). Compared to GO, there is no decrease in fluorescence intensity of GOEE until pH 6–7 due to the missing carboxy acid functionality.

In conclusion, we have demonstrated that the fluorescence properties of GO is highly pH dependent. Fluorescence is strongest at 470 nm excitation and 555 nm emission. The fluorescence intensity is a function of pH but not of temperature and oxygen concentration. Conceivably, GO may be used to sense pH values in cells and related samples. The changes in fluorescence observed with changes in pH do not depend on the excitation/emission wavelength. This makes it a probe that is compatible with all (kinds of) light sources and filter combinations between 300 and 500 nm, e.g. in imaging applications with microscopes. Interference with a second label (e.g. a temperature probe) can be avoided by switching to a suitable wavelength. New functional groups and even whole molecules, e.g. receptors may be added to GO by relatively simple chemistry [20]. This opens the possibility of designing new optical probes and provides a tool for the (nano)design of optical sensor systems based on measurement of either fluorescence intensity, the efficiency of quenching, and of energy transfer. Combination with electrical methods like conductometry, amperometry or potentiometry for opto-electronic devices is also possible.

Acknowledgement The work was performed within the frame of the Graduate College 1570 funded by the DFG (Deutsche Forschungsgemeinschaft).

References

1. Allen MJ, Tung VC, Kaner RB (2010) Honeycomb carbon: a review of graphene. Chem Rev 110(1):132–145. doi:10.1021/cr900070d, pMID: 19610631.
2. Bolotin K, Sikes K, Jiang Z, Klima M, Fudenberg G, Hone J, Kim P, Stormer H (2008) Ultrahigh electron mobility in suspended graphene. Solid State Commun 146(9–10):351–355. doi:10.1016/j.ssc.2008.02.024
3. Özyilmaz B, Jarillo-Herrero P, Efetov D, Abanin DA, Levitov LS, Kim P (2007) Electronic transport and quantum hall effect in bipolar graphene p-n-p junctions. Phys Rev Lett 99(16):166804. doi:10.1103/PhysRevLett.99.166804
4. Schedin F, Geim AK, Morozov SV, Hill EW, Blake P, Katsnelson MI, Novoselov KS (2007) Detection of individual gas molecules adsorbed on graphene. Nat Mater 6(9):652–655. doi:10.1038/nmat1967
5. Qazi M, Vogt T, Koley G (2007) Trace gas detection using nanostructured graphite layers. Appl Phys Lett 91(23): 233101–233103. doi:10.1063/1.2820387
6. Zhu Y, Murali S, Cai W, Li X, Suk JW, Potts JR, Ruoff RS (2010) Graphene and graphene oxide: synthesis, properties, and applications. Adv Mater 22(35):3906–3924. doi:10.1002/adma.201001068
7. Lu CH, Yang HH, Zhu CL, Chen X, Chen GN (2009) A graphene platform for sensing biomolecules. Angew Chem 121(26):4879–4881. doi:10.1002/ange.200901479
8. Sun X, Liu Z, Welsher K, Robinson J, Goodwin A, Zaric S, Dai H (2008) Nano-graphene oxide for cellular imaging and drug delivery. Nano Research 1:203–212. doi:10.1007/s12274-008-8021-8
9. Luo Z, Vora PM, Mele EJ, Johnson ATC, Kikkawa JM (2009) Photoluminescence and band gap modulation in graphene oxide. Appl Phys Lett 94(11):111,909–3. doi:10.1063/1.3098358
10. Bonaccorso F, Sun Z, Hasan T, Ferrari AC (2010) Graphene photonics and optoelectronics. Nat Photon 4(9):611–622. doi:10.1038/nphoton.2010.186
11. Loh KP, Bao Q, Eda G, Chhowalla M (2010) Graphene oxide as a chemically tunable platform for optical applications. Nat Chem 2(12):1015–1024. doi:10.1038/nchem.907
12. Dikin DA, Stankovich S, Zimney EJ, Piner RD, Dommett GHB, Evmenenko G, Nguyen ST, Ruoff RS (2007) Preparation and characterization of graphene oxide paper. Nature 448(7152):457–460. doi:10.1038/nature06016
13. Pan D, Zhang J, Li Z, Wu M (2010) Hydrothermal route for cutting graphene sheets into blue-luminescent graphene quantum dots. Adv Mater 22(6):734–738. doi:10.1002/adma.200902825
14. Eda G, Lin YY, Mattevi C, Yamaguchi H, Chen HA, Chen IS, Chen CW, Chhowalla M (2010) Blue photoluminescence from chemically derived graphene oxide. Adv Mater 22(4):505–509. doi:10.1002/adma.200901996
15. Chen JL, Yan XP (2011) Ionic strength and ph reversible response of visible and near-infrared fluorescence of graphene oxide nanosheets for monitoring the extracellular ph. Chem Commun 47(11):3135–3137. doi:10.1039/C0CC03999C
16. Hummers WS, Offeman RE (1958) Preparation of graphitic oxide. J Am Chem Soc 80(6):1339–1339. doi:10.1021/ja01539a017
17. Liu Z, Robinson JT, Sun X, Dai H (2008) PEGylated nanographene oxide for delivery of water-insoluble cancer drugs. J Am Chem Soc 130(33):10876–10877. doi:10.1021/ja803688x
18. Si Y, Samulski ET (2008) Synthesis of water soluble graphene. Nano Lett 8(6):1679–1682. doi:10.1021/nl080604h
19. Pimenta MA, Dresselhaus G, Dresselhaus MS, Cancado LG, Jorio A, Saito R (2007) Studying disorder in graphite-based systems by raman spectroscopy. Phys Chem Chem Phys 9(11):1276–1290. doi:10.1039/B613962K
20. Dreyer DR, Park S, Bielawski CW, Ruoff RS (2010) The chemistry of graphene oxide. Chem Soc Rev 39(1):228–240. doi:10.1039/B917103G

21. Zhao GJ, Liu JY, Zhou LC, Han KL (2007) Site-selective photoinduced electron transfer from alcoholic solvents to the chromophore facilitated by hydrogen bonding: a new fluorescence quenching mechanism. J Phys Chem B 111(30):8940–8945. doi:10.1021/jp0734530
22. Inoue H, Hida M, Nakashima N, Yoshihara K (1982) Picosecond fluorescence lifetimes of anthraquinone derivatives. radiationless deactivation via intra- and intermolecular hydrogen bonds. J Phys Chem 86(16):3184–3188. doi:10.1021/j100213a024
23. Zuluaga AF, Utzinger U, Durkin A, Fuchs H, Gillenwater A, Jacob R, Kemp B, Fan J, Richards-Kortum R (1999) Fluorescence excitation emission matrices of human tissue: A system for in vivo measurement and method of data analysis. Appl Spectrosc 53(3):302–311. http://as.osa.org/abstract.cfm?URI=as-53-3-302
24. Wolfbeis OS, Leiner M (1985) Mapping of the total fluorescence of human blood serum as a new method for its characterization. Anal Chim Acta 167:203–215. doi:10.1016/S0003-2670(00)84422-0
25. Patra D, Mishra AK (2002) Study of diesel fuel contamination by excitation emission matrix spectral subtraction fluorescence. Anal Chim Acta 454(2):209–215. doi:10.1016/S0003-2670(01)01568-9
26. Bugden J, Yeung C, Kepkay P, Lee K (2008) Application of ultraviolet fluorometry and excitation-emission matrix spectroscopy (eems) to fingerprint oil and chemically dispersed oil in seawater. Mar Pollut Bull 56(4):677–685. doi:10.1016/j.marpolbul.2007.12.022
27. Baker A (2001) Fluorescence excitation-emission matrix characterization of some sewage-impacted rivers. Environ Sci Technol 35(5):948–953. doi:10.1021/es000177t
28. Coble PG (1996) Characterization of marine and terrestrial dom in seawater using excitation-emission matrix spectroscopy. Mar Chem 51(4):325–346. doi:10.1016/0304-4203(95)00062-3
29. Berberan-Santos MN, Garcia JMM (1996) Unusually strong delayed fluorescence of c70. J Am Chem Soc 118(39):9391–9394. doi:10.1021/ja961782s
30. Nagl S, Baleizão C, Borisov SM, Schäferling M, Berberan-Santos MN, Wolfbeis OS (2007) Optical sensing and imaging of trace oxygen with record response. Angew Chem, Int Ed 46(13):2317–2319. doi:10.1002/anie.200603754
31. Wang F, Dukovic G, Brus LE, Heinz TF (2004) Time-resolved fluorescence of carbon nanotubes and its implication for radiative lifetimes. Phys Rev Lett 92(17):177401. doi:10.1103/PhysRevLett.92.177401
32. Barone PW, Baik S, Heller DA, Strano MS (2005) Near-infrared optical sensors based on single-walled carbon nanotubes. Nat Mater 4(1):86–92. doi:10.1038/nmat1276
33. Wang X, Cao L, Yang ST, Lu F, Meziani M, Tian L, Sun K, Bloodgood M, Sun YP (2010) Bandgap-like strong fluorescence in functionalized carbon nanoparticles. Angew Chem 122(31):5438–5442. doi:10.1002/ange.201000982
34. Baker S, Baker G (2010) Luminescent carbon nanodots: emergent nanolights. Angew Chem, Int Ed 49(38):6726–6744. doi:10.1002/anie.200906623
35. Cao L, Wang X, Meziani MJ, Lu F, Wang H, Luo PG, Lin Y, Harruff BA, Veca LM, Murray D, Xie SY, Sun YP (2007) Carbon dots for multiphoton bioimaging. J Am Chem Soc 129(37):11318–11319. doi:10.1021/ja0735271
36. Ray SC, Saha A, Jana NR, Sarkar R (2009) Fluorescent carbon nanoparticles: synthesis, characterization, and bioimaging application. J Phys Chem C 113(43):18546–18551. doi:10.1021/jp905912n
37. Jung J, Cheon D, Liu F, Lee K, Seo T (2010) A graphene oxide based immuno-biosensor for pathogen detection. Angew Chem 122(33):5844–5847. doi:10.1002/ange.201001428